Colloids and Surfaces A 579 (2019) 123658

Contents lists available at ScienceDirect

Colloids and Surfaces A

journal homepage: www.elsevier.com/locate/colsurfa

Synthesis of new chitosan-glutaraldehyde scaffolds for tissue engineering using Schiff reactions

Gabriela Martínez-Mejía[a], Nadia Adriana Vázquez-Torres[b], Andrés Castell-Rodríguez[b], José Manuel del Río[c], Mónica Corea[c,*], Rogelio Jiménez-Juárez[a,*]

[a] Departamento de Química Orgánica, Instituto Politécnico Nacional, Escuela Nacional de Ciencias Biológicas, Prolongación de Carpio y Plan de Ayala S/N, Miguel Hidalgo, C.P. 11340, Ciudad de México, Mexico

[b] Departamento de Biología Celular y Tisular, Universidad Nacional Autónoma de México, Facultad de Medicina, Circuito interior, Ciudad Universitaria, Av. Universidad 3000, C.P. 04510, Ciudad de México, Mexico

[c] Departamento de Nanociencias y Micro-Nanotecnologías, Instituto Politécnico Nacional, Escuela Superior de Ingeniería Química e Industrias Extractivas, San Pedro Zacatenco, Gustavo A. Madero, C.P. 07738, Ciudad de México, Mexico

GRAPHICAL ABSTRACT

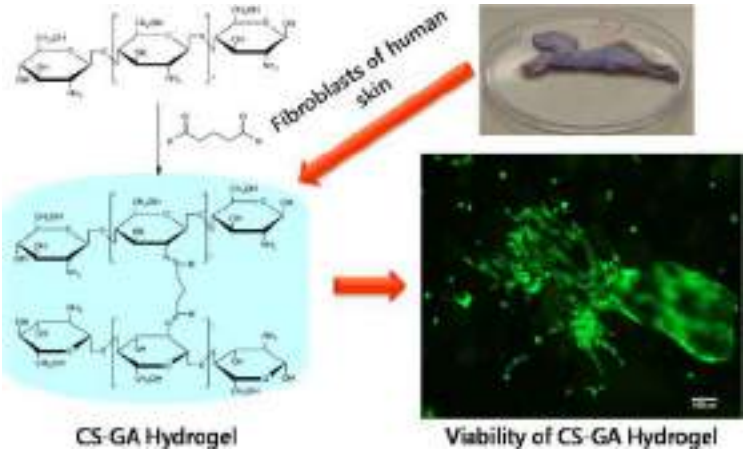

ARTICLE INFO

Keywords:
Hydrogels
Chitosan
Glutaraldehyde
Schiff reaction
Imine
Tissue engineering

ABSTRACT

Hydrogels of chitosan (CS) and glutaraldehyde (GA) were synthesized for tissue engineering applications by using a Schiff reaction. CS was reacted with GA (a cross-linker) at different concentrations, which were expressed as percentage of weight (2, 4, 6, 8 and 10 wt%). An evaluation was made of the effect of the different wt% of GA on the swelling and rheological properties of the hydrogels. The Schiff crosslinking reaction was monitored by UV–vis spectroscopy (550 nm) to determine the reaction kinetics and reaction order at 60 °C. The hydrogel structures were characterized by NMR, FT-IR, HR-MS and SEM, while the degree of cross-linking was examined with TGA-DA. The smaller pores and greatest swelling were found in hydrogels containing 10 wt% of GA. However, only the hydrogels with GA at 2, 4 and 6 wt% displayed viable cells, indicating their *in vitro* cyto-compatibility. The rheological studies showed that the values of the loss and storage modules in the hydrogels

Abbreviations: CS, chitosan; GA, glutaraldehyde; DNP, 2,4-dinitrophenylhydrazine; wt%, percentage of weight; UV-vis, ultraviolet-visible spectroscopy; FT-IR, Fourier-transform infrared spectroscopy; SEM, scanning electron microcopy; DA-TGA, derivate thermogravimetric analysis

* Corresponding authors.
E-mail addresses: mcoreat@yahoo.com (M. Corea), rogeliojj@gmail.com (R. Jiménez-Juárez).

https://doi.org/10.1016/j.colsurfa.2019.123658
Received 31 March 2019; Received in revised form 3 July 2019; Accepted 8 July 2019
Available online 13 July 2019
0927-7757/

increased with a rise in temperature from 30 to 35 and finally 40 °C. Further research is needed to verify the adequacy of these hydrogels as a scaffold for tissue engineering *in vivo*.

1. Introduction

The development of appropriate scaffolds for tissue engineering is still one of the most important fields in regenerative medicine. [1] Creating scaffolds with the appropriate physicochemical factors to sustain cell growth and tissue formation allows regenerative medicine to improve, restore or replace the biological functions of damaged tissues and organs [2]. The scaffolds should serve as templates to guide adhesion, proliferation, differentiation and cell maturation. Furthermore, they must provide the cells with a free space for vascularization, penetration and transfer of nutrients, oxygen and waste products. [1,3] In other words, the scaffolds need to have appropriate mechanical properties and porous structures that permit the free diffusion of nutrients and waste. Also, the degradation process rate should be equal to the cellular growth rate. [4,5] Essentially, scaffolds serve as an artificial extracellular matrix to offer structural support for the cells and free space for the flow of growth factors. The extracellular matrix consists of a crosslinked mesh between fibrous proteins and glycosaminoglycans (GAGs, such as heparan sulfate, chondroitin sulfate and keratan sulfate) to form proteoglycans. [6]

Materials used as scaffolds include hydrogels, porous nanostructures and nanofibers. [[7]] Hydrogels are three-dimensional polymer networks able to swell and absorb a large amount of aqueous solution without losing their structure [8–10]. They can retain solvent representing at least 20% of their own weight and swell significantly by absorbing water, followed by shrinking again after de-swelling. However, the process of cross-linking creates an insoluble network [11,12].

Several monomers and crosslinking agents have been employed to synthesize hydrogels with a wide range of chemical compositions, many of which could possibly serve as scaffolds [13,14]. There are several routes for the synthesis of these platforms, including Michael, Click and Schiff reactions. A Michael reaction involves the nucleophilic addition of a carbanion or a nucleophile (e.g., thiols and amines) to create a reaction with an <,® unsaturated carbonyl compound [15]. A Click reaction consists of a Cu(I)-catalyzed reaction between azide and terminal acetylene groups to form 1,2,3-triazoles [16]. Finally, a Schiff reaction is generated by the condensation of ketone or aldehyde groups and a primary amine [17]. The synthesis process begins with an intermediate of carbonylamine, which upon dehydration forms a carbon-nitrogen double bond (an imine). These methods present advantages and disadvantages for controlling the formation of the hydrogel structure. For instance, some functional groups may not react during the crosslinking reaction, thus resulting in hydrogels with poor mechanical properties [13].

Hence, it is important to choose the type of reaction that is adequate for each particular polymer. For example, chitosan (CS) has been used for the preparation of hydrogels via the Schiff base reaction [5–7]. CS is a linear heteropolymer of glucosamine and N-acetyl glucosamine residues (Fig. 1] that is obtained by the deacetylation of chitin. This weak base is soluble in acidic solution (pH 6.5) and insoluble in water and organic solvents [18–22]. It is biodegradable, biocompatible and non-toxic and exhibits mucoadhesive properties [23]. In the current study, synthesis was carried out of a series of hydrogels with various concentrations of glutaraldehyde (GA). The content of GA is expressed as its percentage of hydrogel weight (wt%), being 2, 4, 6, 8 and 10 wt%. The reaction conversion of GA was monitored by ultraviolet-visible spectroscopy (Uv–vis) and the reaction order was calculated from the corresponding data. The materials were characterized by Fourier-transform infrared spectroscopy (FT-IR), scanning electron microscopy (SEM) and thermogravimetry (TGA). The degree of cross-linking of the hydrogels was determined by Soxhlet techniques, the rheological properties such as loss and storage modulus were measured, and cell viability was evaluated with a cytotoxicity assay.

2. Materials and methods

2.1. Materials

CS (75% deacetylated) and 2,4-dinitrophenylhydrazine (DNP) (99%) were obtained from Sigma-Aldrich (Iceland), 99% acetic acid from J.T. Baker (Mexico), ethanol and dichloromethane from Alveg (Mexico), and 25 wt.% GA from Merck (Germany). Distilled water grade II was used as solvent. The high glucose Dulbecco's modified Eagle's medium (DMEM), antibiotic-antimitotic 100X and fetal bovine serum (FBS) were purchased from Biowest (Mexico). Trypsin/EDTA solution and phosphate buffed saline (PBS, pH 7.4) were acquired from Gibco (Mexico). Calcein AM and ethidium homodimer (EthD-1) were provided by Life Technologies (USA).

2.2. Chitosan scaffold synthesis

The synthesis of CS scaffolds (Scheme 1) began by dissolving 0.03 g CS **2** in 1% acetic acid aqueous solution. Different aliquots (0.05, 0.1, 0.15, 0.20 and 0.25 mL) of GA **3** (1.25% aqueous solution) were added drop wise and the reaction mixture was stirred for 2 h at 60 °C. Assays were performed in triplicate.

2.2.1. Reaction kinetics of chitosan and glutaraldehyde

The reaction between CS and GA was monitored by UV–vis spectroscopy at 550 nm in a PerkinElmer Lamda 25 UV–vis double beam spectrophotometer (Model 643, USA), taking samples every 5 min. Samples were extracted with methylene chloride under vigorous agitation, and then 2 mL of ethanol and 2 mL 2,4-dinitrophenylhydrazine of acid alcoholic solution (DNP) were added to the organic phase and the mixture was stirred. [24] The samples were analyzed by UV–vis spectroscopy. Data were interpolated by a previously elaborated calibration curve to determine the concentration of residual GA during the crosslinking reaction (Supplementary materials). In this way, the GA conversion was tracked during the reaction between residual GA **1** and DNP **2** (Scheme 2).

The calibration curve was prepared by using seven solutions of different concentrations of 2,4-dinitrophenylhydrazone. The compound was obtained by reacting 1.0 equiv. of GA and 2.0 equiv. of DNP following the aforementioned procedure (Table 1, Fig. 2). The experiments were performed by triplicate.

2.2.2. Freeze-drying

The hydrogels obtained were freeze-dried in stages in a Labconco (S/M Series FJMJ98, USA) lyophilizer. The first freezing step took place at −10 °C for 30 min. Afterwards, a vacuum of up to 89×10^{-3} mBars

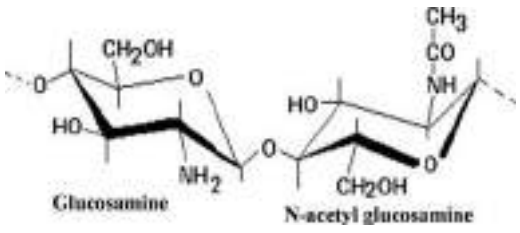

Fig. 1. Chemical structure of chitosan.

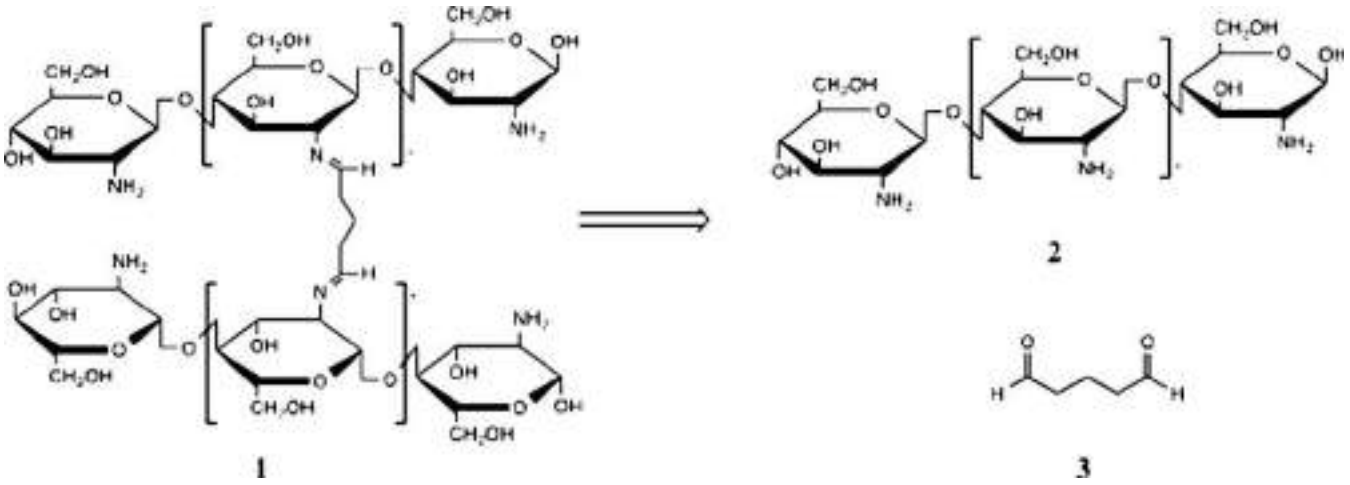

Scheme 1. Retrosynthetic scheme 1. Crosslinked hydrogels of chitosan-glutaraldehyde.

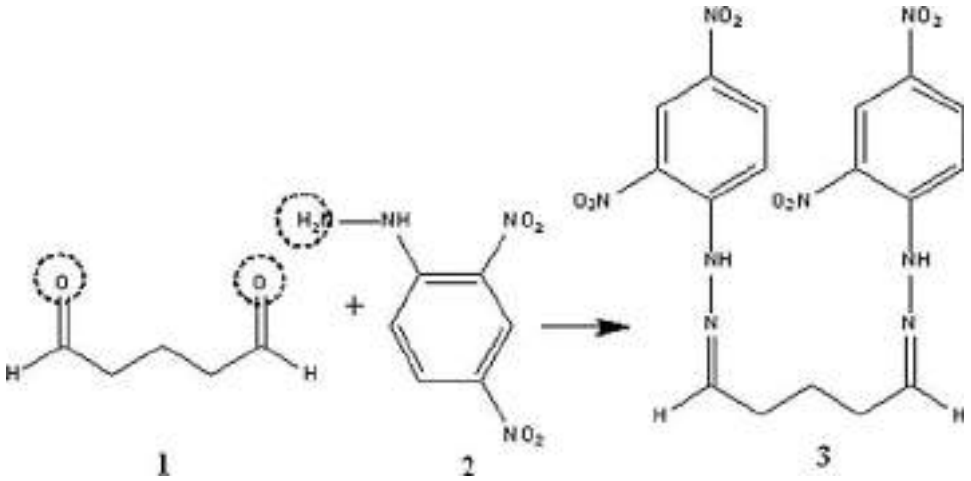

Scheme 2. Reaction scheme of the aldehyde identification test.

Table 1
Dilutions used for the calibration curve.

GA (g)	DNFH (g)
0.0000	0.0000
0.0007	0.0028
0.0014	0.0056
0.0021	0.0085
0.0029	0.0113
0.0036	0.0141
0.0043	0.0170
0.0050	0.0198

was applied and the second thermal stage of -46 ± 0.1 °C lasted 1.5 h. Finally, the temperature was elevated to 30 ± 0.1 °C and maintained for 1.5 h.

2.2.3. Spectroscopic techniques

One-dimensional (1D) ^{1}H-NMR and ^{13}C-NMR spectra were recorded at 499.85 MHz on a Varian (now Agilent) NMR System 500 spectrometer (Agilent Technologies, Inc., Santa Clara, CA, USA). Samples of 30 mg hydrogel with GA at 10 wt% as well as its uncrossed fraction were dissolved in deuterated acetic acid/deuterated water (D_2O) (1:1). The non-crosslinked part of polymer was extracted washing the hydrogels by Soxhlet techniques using ethyl acetate as solvent. The ^{1}H-NMR spectra were recorded by employing a PRESAT pulse sequence to suppress the residual H_2O signal. As a reference for the ^{1}H NMR chemical shifts, the signals of non-deuterated solvent residues were set at δ = 11.65 ppm and 4.79 ppm for acetic acid and water, respectively. For ^{13}C NMR, the signals were set at δ = 178.99 ppm and 22.44.0 ppm for acetic acid.

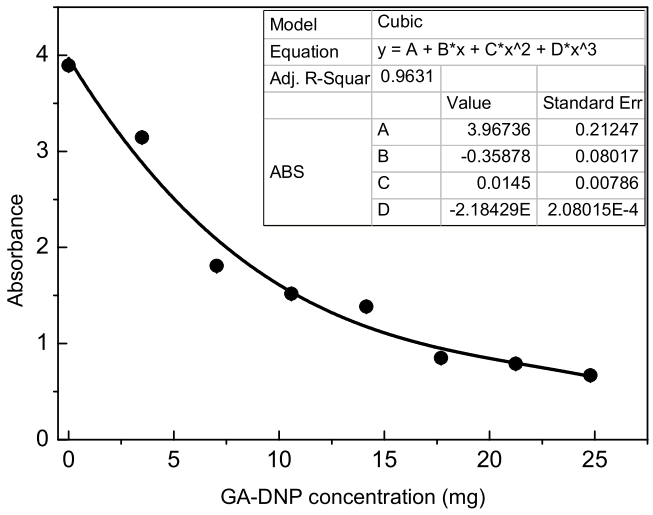

Fig. 2. Calibration curve for the GA-DNP complex.

Fresh hydrogels were analyzed by Fourier-transform infrared

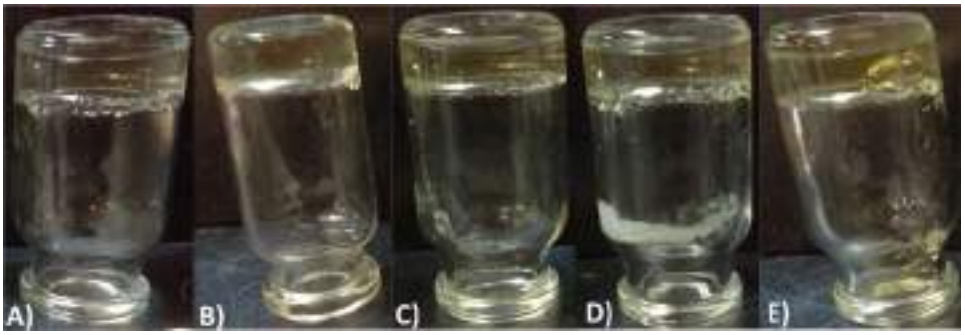

Fig. 3. Photographs of crosslinked hydrogels with different concentrations of GA: A) 2 wt%, B) 4 wt%, C), 6 wt%, D) 8 wt% and E) 10 wt%.

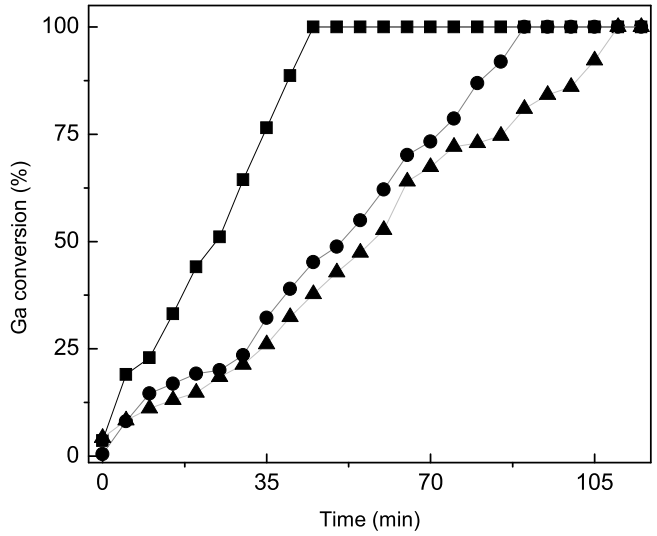

Fig. 4. GA conversion as a function of time for hydrogels with this crosslinking agent at 2 wt% (■), 6 wt% (●) and 10 wt% (▲).

spectroscopy (FT-IR) on a Perkin-Elmer infrared spectrophotometer (Model 720 X, USA) using a double beam. The apparatus was equipped with attenuated total reflectance in the range of 400 to 4000 cm^{-1}. Fresh hydrogels were also examined by high-resolution mass spectrometry (HR-MS) on a mass spectrophotometer with micrOTOF II-Q and electrospray ionization (BrukerDaltonisc, Billerica, MA, USA).

2.2.4. Degree of cross-linking

Gel samples were washed with ethyl acetate in a Soxhlet extractor until achieving a constant weight. The degree of cross-linking (*D*) was calculated gravimetrically by the following Eq. (1):

$$\%D = \frac{W_g}{W_0}\text{x}100 \quad (1)$$

where W_g is the sample weight after the wash and W_0 is the initial mass.

Table 2
Reaction order and reaction rates of the crosslinked hydrogels at 60 °C.

Hydrogel	k (kg/s)	r
2%	1.38×10^{-10}	0.9919
4%	9.45×10^{-11}	0.9769
6%	9.83×10^{-11}	0.9864
8%	1.11×10^{-10}	0.9934
10%	1.11×10^{-10}	0.9885

2.2.5. Thermogravimetric analysis

Derivate thermogravimetric analysis (DA-TGA) of the hydrogels was carried out on a 6000 PerkinElmer simultaneous thermal analyzer (Germany). The samples were heated from 25 to 500 °C at a rate of 10 °C/min under nitrogen atmosphere.

2.2.6. Rheological analysis

Rheological properties were evaluated with a Modular Compact Rheometer (model MCR 502, Anton Paar, Austria) using PP25 parallel plate geometry (25 mm diameter, 0°). Samples were placed in the center of the bottom plate. The upper plate was immediately lowered to a gap of 1 mm and the measurement was performed. The analysis was made at 30, 35 and 40 °C.

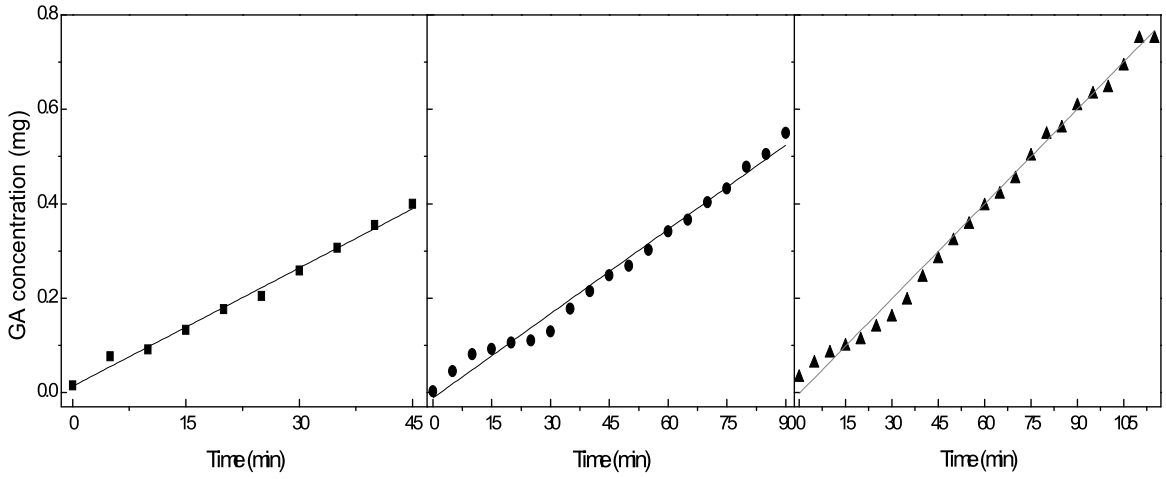

Fig. 5. Reaction order for hydrogels with glutaraldehyde at 2 wt% (■), 6 wt% (●) and 10 wt% (▲).

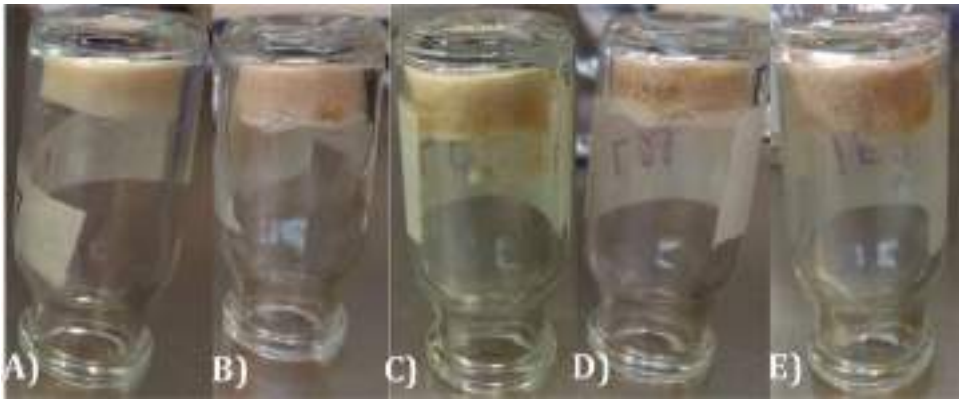

Fig. 6. Freeze-dried hydrogels with different concentrations of the crosslinking agent (glutaraldehyde): A) 2 wt%, B) 4 wt%, C), 6 wt%, D) 8 wt% and E) 10 wt%.

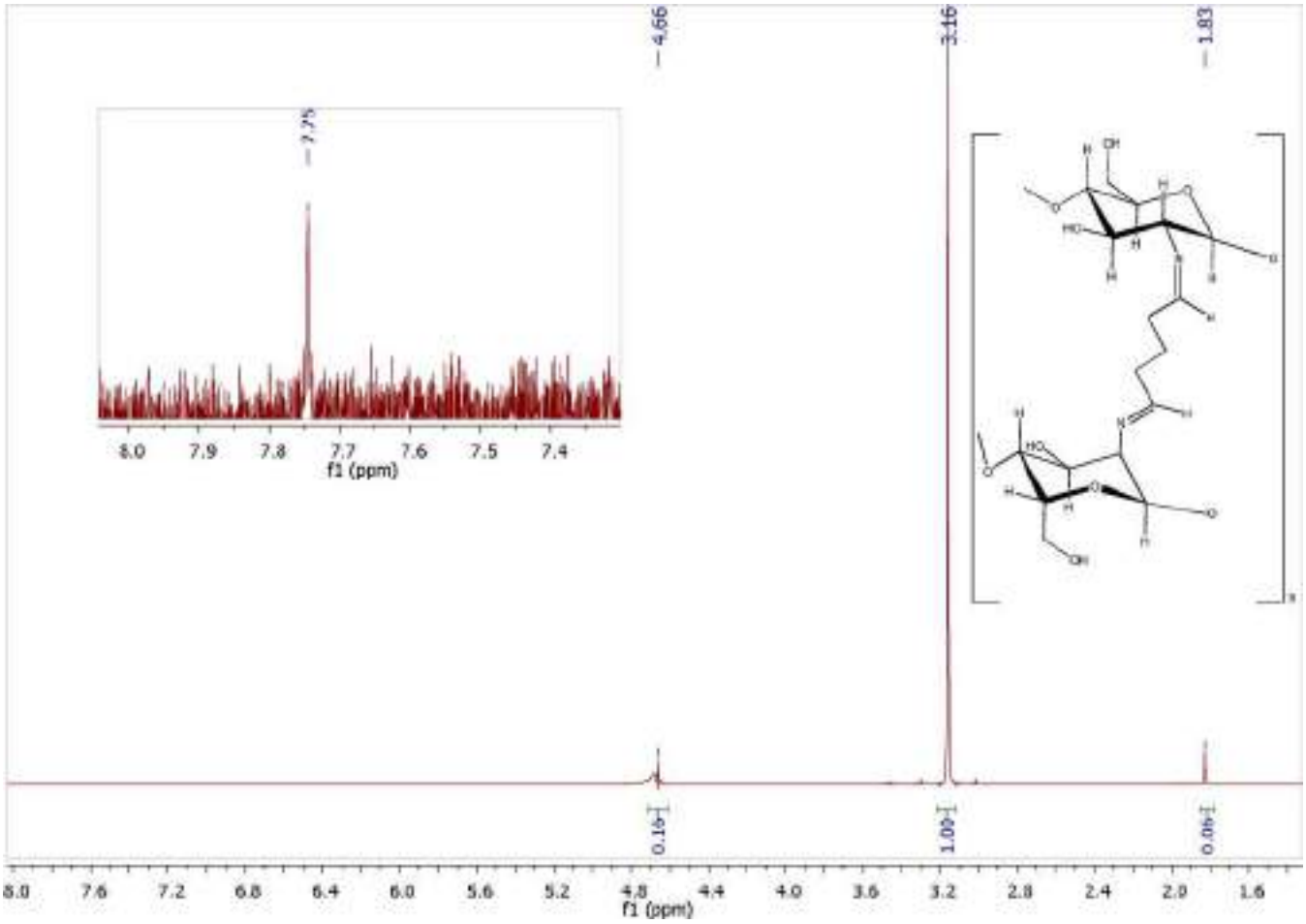

Fig. 7. ^{1}H NMR of hydrogel at 10 wt%.

2.2.7. Scanning electron microscopy (SEM)

Surface morphologies and crosslinking sections of the CS scaffolds were frozen with liquid nitrogen and a vacuum was applied for 24 h. Subsequently, they were covered with gold and observed on a JEOL JSM 6400 field-emission scanning electron microscope (USA) at 5 kV.

2.2.8. Swelling

Hydrogel samples (50 mg) were prepared in a mesh and submerged in distilled water at room temperature. A hydrogel sample was taken at several time intervals, the water removed, and the hydrogels weighed. The swelling ratio (S) of hydrogels as a function of time was calculated from the following Eq. (2):

$$S(\%) = \frac{W_t}{W_i} x100 \quad (2)$$

where W_t is the sample weight after recovery and W_i is initial mass.

2.2.9. Cytotoxicity assay

For testing the capacity of the scaffolds to support cell growth, primary cultures of human fibroblasts were used. These cells were obtained from the skin of healthy donors with prior informed consent. The biopsies had a size of 4 mm in diameter. Hydrogels were previously washed with NaOH solution (1 N) and distilled water to establish a pH close to 7.4 and eliminate traces of GA. In order to demonstrate that GA

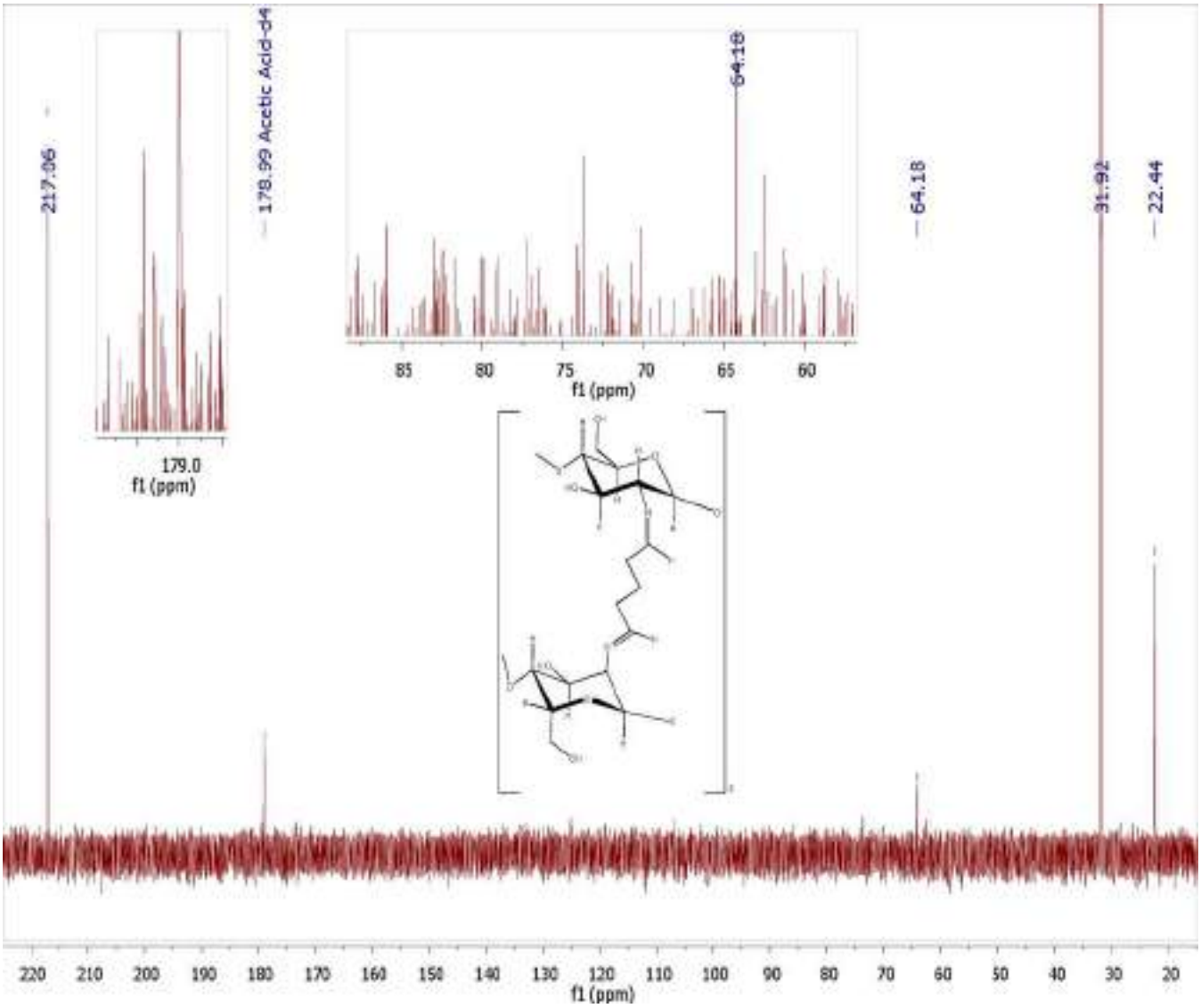

Fig. 8. ^{13}C NMR of the hydrogel with GA at 10 wt%.

traces were removed in the washes, ^{1}H-NMR was running as a qualitative analysis in methanol-d4/D_2O solvent on Bruker spectrophotometer and quantitatively by UV–vis spectroscopy at 550 nm in a PerkinElmer Lamda 25 UV–vis double beam spectrophotometer with 2,4-dinitrophenylhydrazine of acid alcoholic solution (DNP). Data were interpolated by a previously elaborated calibration curve.

Thin layers samples of hydrogels were put on 0.5 x 0.5 mm coverslip frames, these were put in 48-well plates and sterilized by UV irradiation. Subsequently, 18 µL of cell suspension in DMEM were seeded onto hydrogel samples (5000 cells per sample) and incubated for 1 h at 37 °C, adding DMEM to the hydrogels. The cell-seeded hydrogels were cultivated for 1 week at 37 °C, changing the medium every 2 days.

After 3 days, the cultivation medium was removed from the wells. The hydrogels were rinsed with PBS solution, stained with 1 mL of calcein/ethidium homodimer solution and incubated for 1 h at 37 °C. With this dye, living cells fluoresce green and the nuclei of dead cells is red, thus providing the basis of the fluorescence live/dead assay. The overall cell morphology was observed by epifluorescence microscopy (Nikon Eclipse 80i, Tokyo, Japan), with an excitation wavelength of 480 nm and an emission wavelength of 520 nm, following the manufacturer's instructions. Cell count was carried out by image analysis.

3. Results and discussion

A series of hydrogels of CS and GA were synthesized (at 60 °C) by means of the Schiff base method, obtaining five concentrations of GA (2, 4, 6, 8 and 10 wt%) and therefore a range in the degree of crosslinking in the polymer. The synthesis was carried out in triplicate. Photographs of the resulting hydrogels (Fig. 3) reveal that all were a transparent yellow in color. This color became more intense as the concentration of the crosslinking agent increased. Gels with lower concentrations of GA presented runoff.

3.1. Reaction kinetics of chitosan and glutaraldehyde

The reaction progress was monitored for each hydrogel at 60 °C. The conversion data of GA as a function of time for hydrogels with a concentration of 2 wt% (■), 6 wt% (●) and 10 wt% (▲) are illustrative of the results (Fig. 4]). The hydrogel containing GA at 2 wt% was completely consumed at 50 min of reaction. For the hydrogel with GA at 10 wt%, this occurred at 120 min of reaction. Hence, there was a faster reaction of GA with CS for hydrogels that had a lower versus higher concentration of the crosslinking agent. Perhaps the crosslinking density affects the diffusion coefficient of the compounds to avoid a fast reaction. [25]

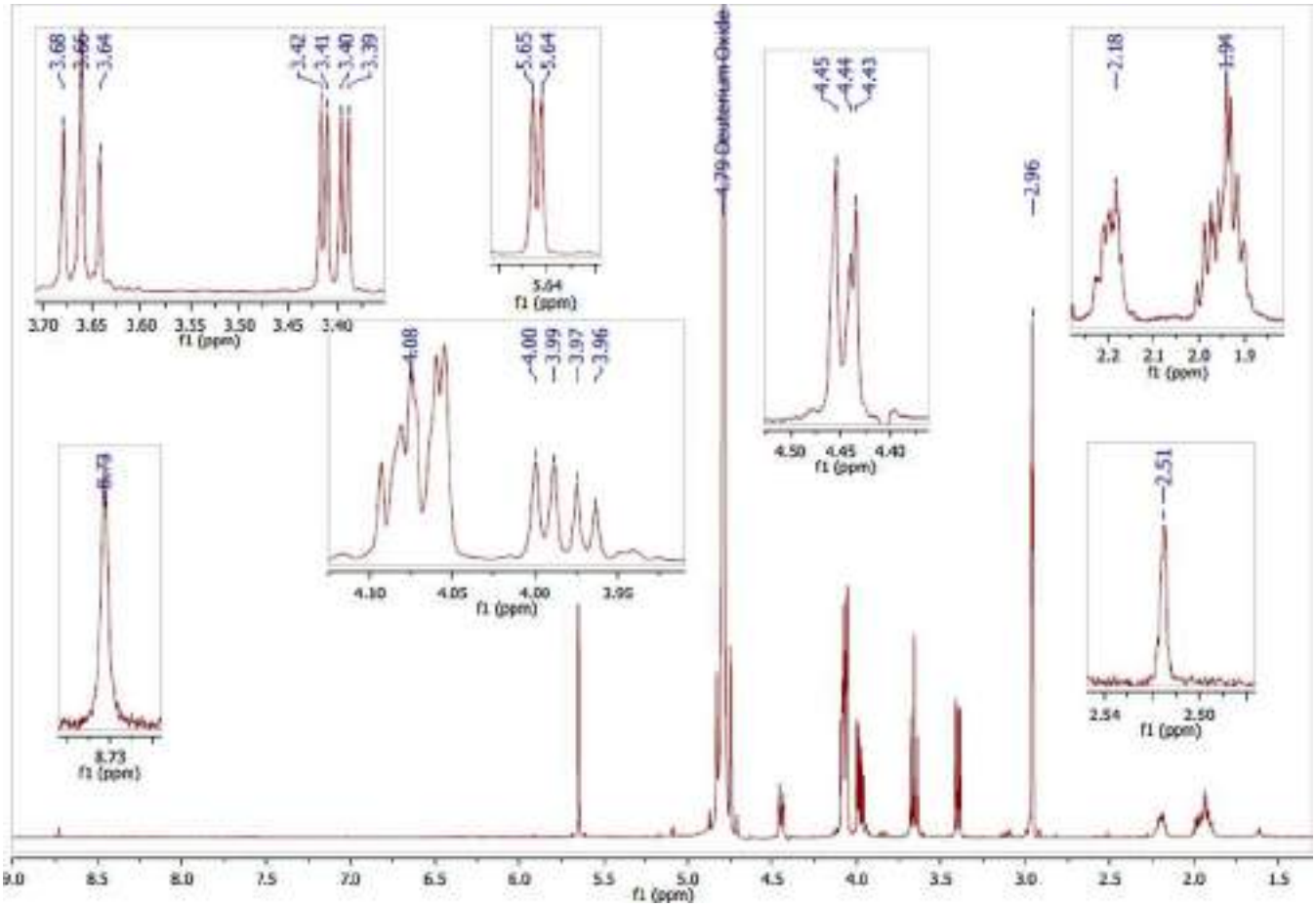

Fig. 9. ^{1}H NMR of the non-crosslinked part of hydrogel with glutaraldehyde at 10 wt%.

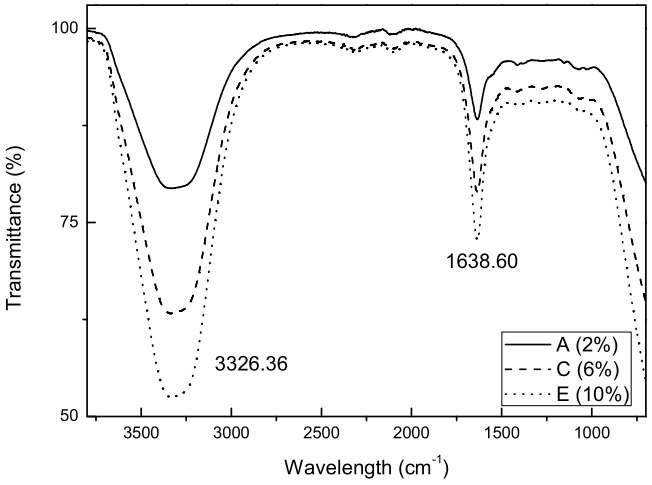

Fig. 10. FT-IR spectra of chitosan-glutaraldehyde hydrogels containing the crosslinking agent at 2 wt%, 6 wt% and 10 wt%.

The reaction order was established from GA conversion data for each hydrogel. The results for hydrogels containing 2 wt% (■), 6 wt% (●) and 10 wt% (▲) of GA (Fig. 5) show that the CS-GA reaction corresponds to a zero-order kinetic. However, the reaction became slower as the concentration of GA increased. Since GA was at a lower concentration than CS in the gel formation, the reaction can be considered to be of pseudo zero order. This coincides with the descriptions by some authors of a spontaneous and immediate reaction [25,10,20].

The reaction rate constants at 60 °C were calculated by the kinetic Eqs. (3) and (4):

$$[GA] = [GA]_0 + k * t \quad (3)$$

$$[GA] = k * t \quad (4)$$

The Pearson index (r) for all rate constants has a value close to 0.98 (Table 2). Additionally, the values of rate constants confirm the results obtained for the reaction progress, because the hydrogel with GA at 2 wt% had the highest rate constant value (1.38×10^{-10} kg/s), while the polymers with a greater degree of cross-linking showed rate constant values close to 1.11×10^{-10} kg/s. The same procedure for determining the reaction order was also used by Liao and co-workers for hydrogels with poly(acrylic acid-co-2-acrylamido-2-methylpropane sulfonic acid) and AA/AMPS [26].

3.2. Freeze-drying

A series of five freeze-dried hydrogels were obtained and photographed (Fig. 6). The light-yellow color was more intense for the hydrogels with greater concentration of the crosslinking agent. The material had a sponge-like appearance and a soft texture. The porosity can be explained by the sublimation of water by lyophilization process.

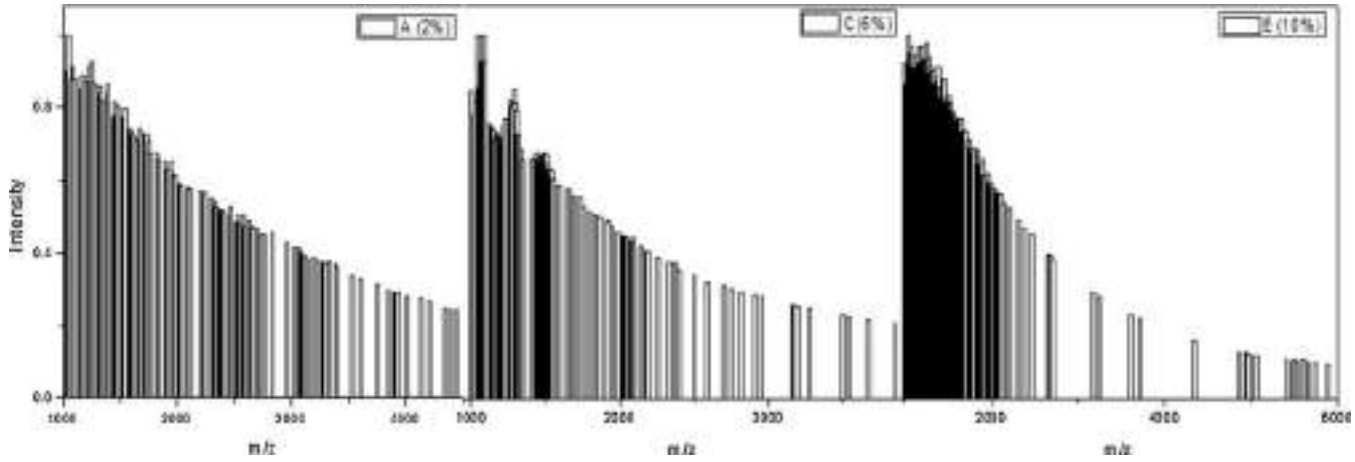

Fig. 11. HR-MS spectra of chitosan-glutaraldehyde hydrogels containing the crosslinking agent at 2 wt%, 6 wt% and 10 wt%.

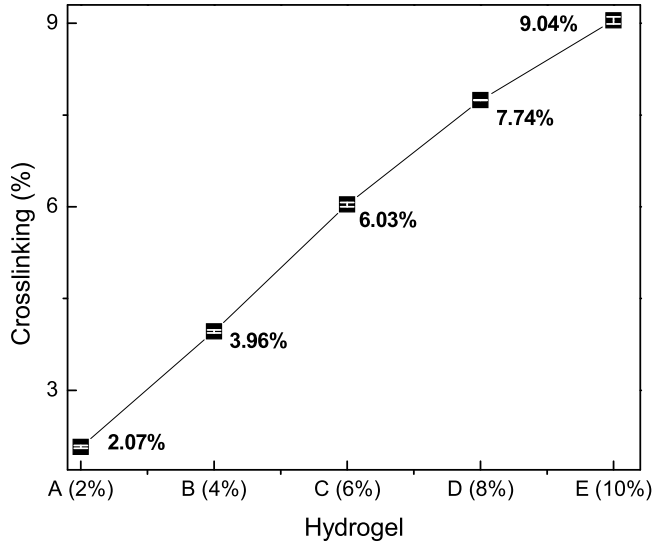

Fig. 12. Degree of chitosan-glutaraldehyde cross-linking in hydrogels containing the crosslinking agent at 2 wt%, 4 wt%, 6 wt%, 8 wt% and 10 wt%.

3.3. Spectroscopic analysis

Spectra of ^{1}H NMR, result shown for the crosslinking in the hydrogel containing GA at 10 wt% (Fig. 7). A signal at $\delta = 7.75$ ppm was attributed to the imine protons for cross-linking between GA and CS (-N = CH-), in agreement with the report by Ali Reza Karimi [17]. A wide signal at $\delta = 4.66$ ppm corresponds to hydroxyl (−OH) groups in the CS chain, $\delta = 3.16$ ppm to oxygen base protons near hydroxyls (OH−CH-), and $\delta = 1.83$ ppm to methylene groups of the cross-linked glutaraldehyde chain.

The hydrogel was also analyzed by ^{13}C NMR, illustrated by the spectrum of the hydrogel with the crosslinking agent at 10 wt% (Fig. 8). The signal at $\delta = 217.06$ ppm corresponds to carbonyl of GA, $\delta = 180$ ppm to the carbonyl of imine (-C = N-), $\delta = 64$ ppm to the nitrogen base carbon (−CH-N=), $\delta = 64.18$ ppm to the oxygen base carbon (−CH-O-) and $\delta = 31.92$ ppm to the methylene groups of the crosslinked GA chain. These results corroborate the formation of crosslinks with imine bonds during the reaction between GA and CS.

The hydrogels were washed by Soxhlet techniques and the non-crosslinked part of polymer was extracted. The ^{1}H NMR spectrum of the non-crosslinked part of the hydrogel containing 10 wt% of GA (Fig. 9) showed a multiplet signal at $\delta = 1.94$ ppm and $\delta = 2.18$ ppm and a signal at $\delta = 8.73$ ppm corresponding to residual GA. The results were corroborated with a spectrum of pure GA, where the same signals

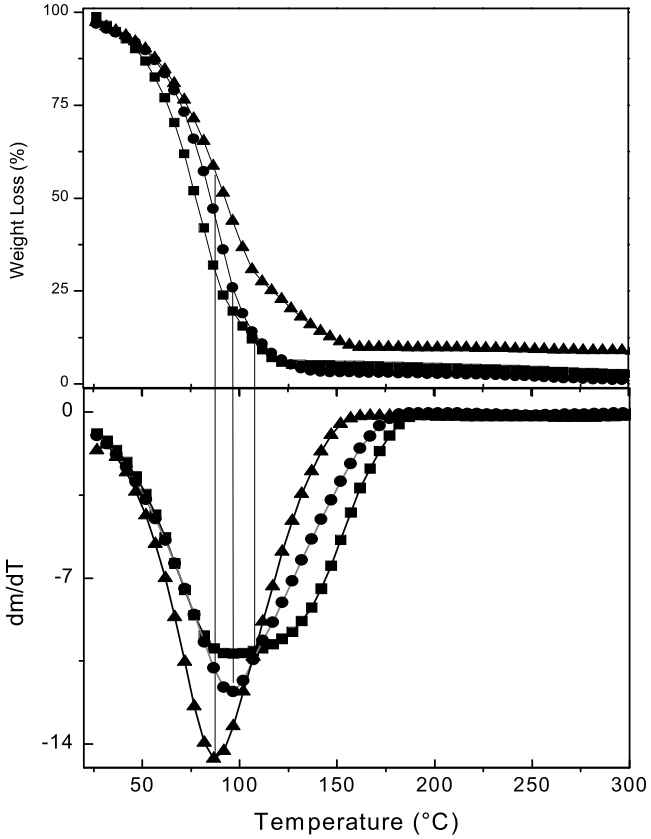

Fig. 13. Plot of the TGA and derivate analyses of crosslinked hydrogels with glutaraldehyde at 2 wt% (■), 6 wt% (●) and 10 wt% (▲).

Table 3
Comparison of the theoretical and calculated percentages of the crosslinking agent.

Theoretical concentration of the crosslinking agent (%)	Concentration of the crosslinking agent by Soxhlet (%)	Concentration of the crosslinking agent by TGA (%)
2	2.07	1.99
4	3.96	3.10
6	6.03	5.46
8	7.74	7.67
10	9.04	9.92

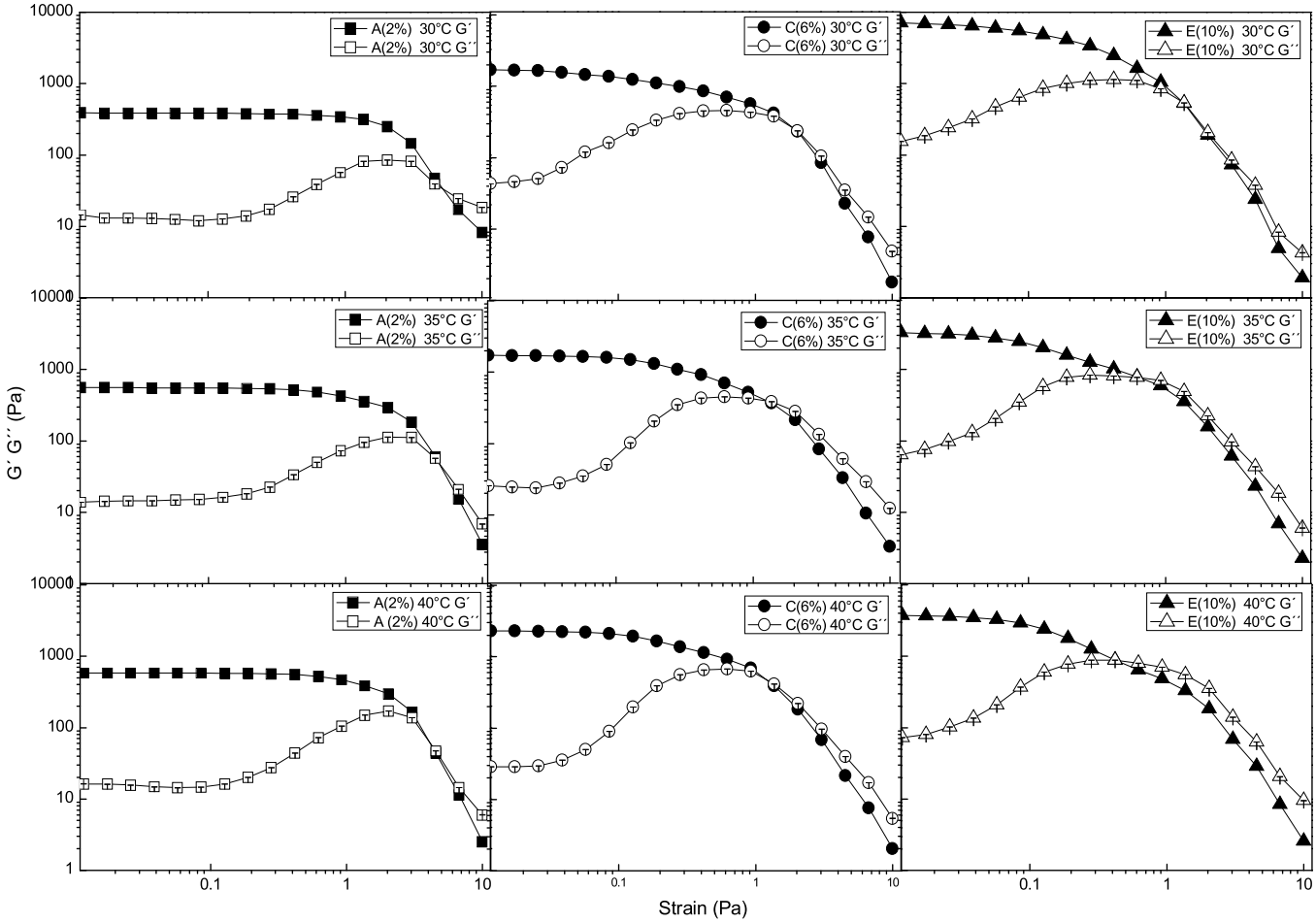

Fig. 14. Rheological behavior of hydrogels with glutaraldehyde at 2 wt% (■), 6 wt% (●) and 10 wt% (▲).

Table 4
Flow points of the hydrogels at different temperatures.

Temperature (°C)	Flow point (Pa)		
	2 wt.%	6 wt.%	10 wt.%
30	5.16	1.98	1.39
35	4.85	1.27	0.65
40	4.04	1.21	0.44

appear. Additionally, there was a quadruplet at $\delta = 3.41$ ppm, a triplet at $\delta = 3.66$ ppm, a quadruplet at $\delta = 3.98$ ppm, a multiplet at $\delta = 4.08$ ppm and a multiplet at $\delta = 4.44$ ppm for residual CS. These signals also coincided with the spectrum of pure glucosamine as well as bibliographical data. [27] Finally, a signal at $\delta = 2.51$ ppm corresponds to residual acetyl methyl groups.

The ^{13}C NMR spectrum of the non-crosslinked part of the hydrogel with GA at 10 wt.% could not be discerned because of the scant amount of compound. The results of NMR confirmed that the non-crosslinked part does not have imine-linkage formation. Moreover, the signals showed the existence of residual CS and GA, and their intensity indicated a lower concentration of GA than CS.

FT-IR analysis was carried out on fresh hydrogels with the crosslinking agent at 2 wt%, 6 wt% and 10 wt% (Fig. 10). The absorption band at 1638 cm^{-1} corresponds to the stretching frequencies of the imine bond (HC = N-), in accordance with a previous study employing the same reaction that assigned the imine group to 1568 cm^{-1}[17] and the overlapped stretching vibration of −N−H and −OH to 3326 cm^{-1}.[17] Both these signals presently increased when there was a greater degree of cross-linking in the hydrogels.

HR-MS reveals a wide distribution of the molecular mass for each hydrogel (Fig. 11). Some chains were found with high molecular weight and others with low molecular weight. The latter are attributed to a slow reaction that does not permit the fast growth of polymeric chains. This evidence corroborates the findings of the NMR spectra, in which residual CS and GA were detected.

3.4. Degree of cross-linking

The degree of cross-linking for each hydrogel, determined by Soxhlet techniques (Fig. 12), closely corresponded to the theoretically calculated concentration of GA for each hydrogel. At the highest concentrations of the crosslinking agent, a decrease in the crosslinking reaction efficiency can be observed. A reduced permeation of the compounds probably occurred due to the enhanced network, meaning that one carbonyl of GA reacts with the amine group of CS while the other is left free. [10] This was corroborated by the resonance results of the non-crosslinked part, which show the presence of non-crosslinked

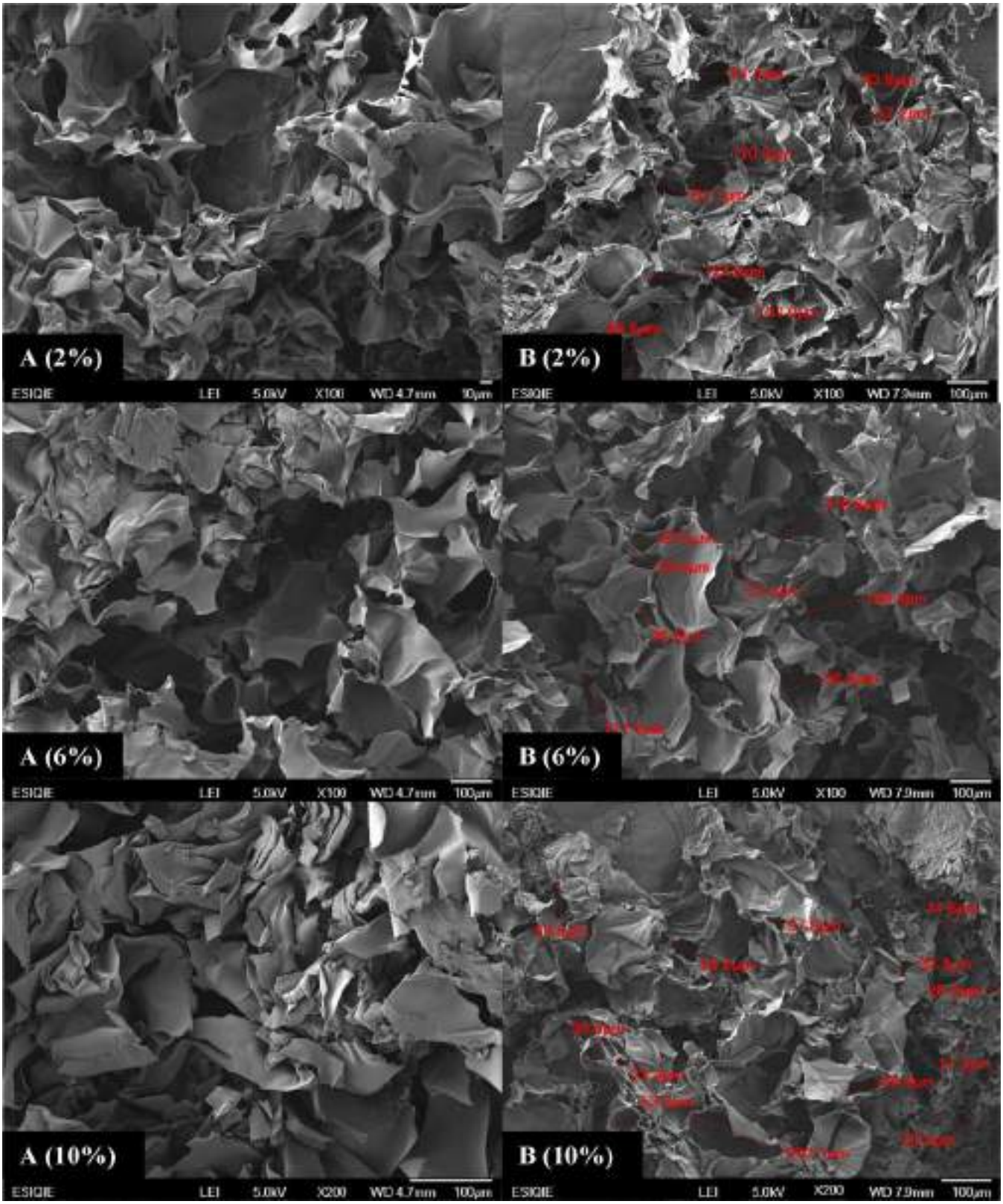

Fig. 15. Microscopy images of the surfaces of hydrogels, both fresh (A) and lyophilized (B), containing 2 wt%, 6 wt% and 10 wt% of the crosslinking agent.

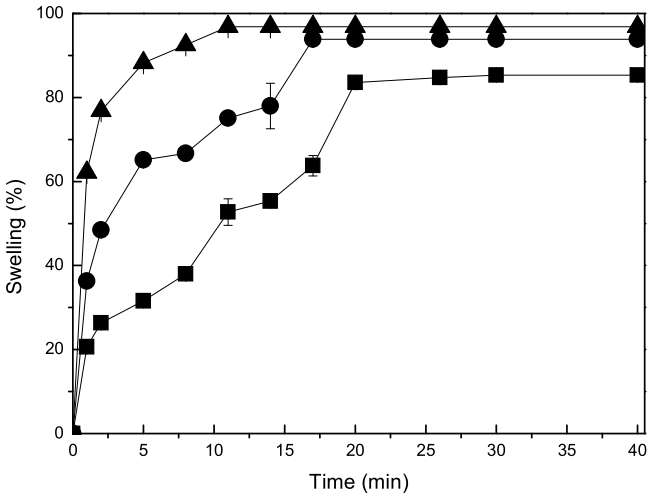

Fig. 16. Swelling of hydrogels with the crosslinking agent at 2 wt% (■), 6 wt% (●) and 10 wt% (▲).

Table 5
The maximum water absorption of the hydrogels.

Hydrogel (%)	Absorbed water (g)/ g of hydrogel
2	5.83
4	10.54
6	15.20
8	20.10
10	30.51

Table 6
Results of residual GA.

Hydrogel washes	GA (mg)
A (2%)	0.0014
B (4%)	0.0045
C (6%)	0.001
D (8%)	0.0195
E (10%)	0.072

GA and CS, and by the kinetic results, which reveal that the hydrogels with the highest concentrations of GA had the lowest values of the rate constant.

3.5. Thermogravimetric analysis

The DA-TGA test indicated that the hydrogel with the greatest concentration of GA decomposed at the highest temperature (Fig. 13), caused by the greater crosslinking density and therefore a higher average molecular weight of the polymer chains.

At first, the hydrogels with GA at 2, 4 and 6 wt.% presented the same weight loss at $25 < T/°C < 52$, attributed to dehydration of the material and the beginning of the decomposition of shorter chains. As the temperature approached 100 °C, there was a faster decomposition of the hydrogels containing GA at 2 and 6 wt.%. On the other hand, the hydrogel with GA at 10 wt.% did not accelerate its decomposition (due to its greater water retention). A more complete explanation is provided in the section on swelling behavior. Finally, the hydrogels having 2 and 4 wt% of the crosslinking agent completely decomposed at a temperature close to 158 °C, exhibiting a weight loss of 1.99% and 5.46%, respectively. Meanwhile, the hydrogel with GA at 10 wt% completely decomposed at nearly 165 °C, showing a final weight loss of about 9.92%. Such a weight loss is similar to the theoretical crosslinking density for each polymer. TGA results demonstrated that the polymer is stable at 37 °C. This is an important factor to take into account for the preparation of hydrogels used as biomaterials, being the temperature at which the regeneration process is normally carried out [14].

The theoretical concentration of the crosslinking agent was compared to that obtained from Soxhlet and thermogravimetry (Table 3). Hence, the experimental and calculated crosslinking densities were similar.

3.6. Rheological analysis

The rheological properties of the hydrogels were studied by oscillatory rheology at 30, 35 and 40 °C. The storage modulus (G´) and loss modulus (G´´) were determined as a function of strain, (Fig. 14), finding that G' was higher than G´´. Thus, the former represents the more elastic response of the sample, which is reportedly typical for gels or samples with a certain rigidity in their structure [28]. The shape of the storage modulus curve at low frequencies is typical of the shape of a polymer with mechanically weak cross-links [29].

The hydrogel containing GA at 2 wt% had a constant elastic modulus until reaching a tension of 1.5 Pa. At this point, a drop in the value of the module occurred due to the loss of storage capacity, which was caused by the deformation of the hydrogel chains. Likewise, the viscous module remained constant until 0.13 Pa. The increase at this point was attributed to the greater energy loss resulting from the deformation of the chains. The next event of interest is the point of crossing of both modules (denominated the flow point), when the hydrogel chains have been completely broken. All the hydrogels showed the same general behavior, but at different points of G' and G". A higher concentration of GA produced greater values for both modules.

Temperature also had an influence on the points of flow (Table 4). A rise in the temperature exacerbated the tension between the chains of a hydrogel, favoring breakage at a low tension. Hence, the hydrogel with GA at 10 wt% had the smallest values for the flow point, since a higher concentration of GA implies more tension in the polymer chains of the network.

3.7. Scanning electron microscopy (SEM)

The morphology of fresh and freeze-dried hydrogels was examined by SEM. Micrographs of the hydrogels containing 2 and 6 wt.% of the crosslinking agent (Fig. 15) show highly porous surfaces and the formation of flakes in fresh (Panel A) and lyophilized (Panel B) gels. There are studies that document the importance of a porous surface for cells to be implanted inside of the hydrogel and for nutrients to be able to flow to such cells, thus enabling tissue growth on the scaffold [3],[30]. Each fold in the gel structure represents the formation of chemical crosslinking, according to Myhie Kim et al. [31].

SEM micrographs revealed that the network in lyophilized hydrogels (Fig. 15) contained interconnected pores varying in size from 30 to 130 μm, which is necessary for the growth of bone cells such as osteoblasts (20–30 μm) and osteoclasts (100 μm). [32] Greater porosity was observed in the lyophilized than fresh materials, apparently because the lyophilization process removed water by sublimation, leaving holes inside the hydrogel. A smaller number of pores existed in hydrogels with a higher versus lower concentration of crosslinking agent. In addition to the number, the size and shape of pores were affected by the amount of GA used. The same conclusion was reached by Ivaylo] Stefanov, who synthesized hydrogels of thiolated CS with gallic acid as

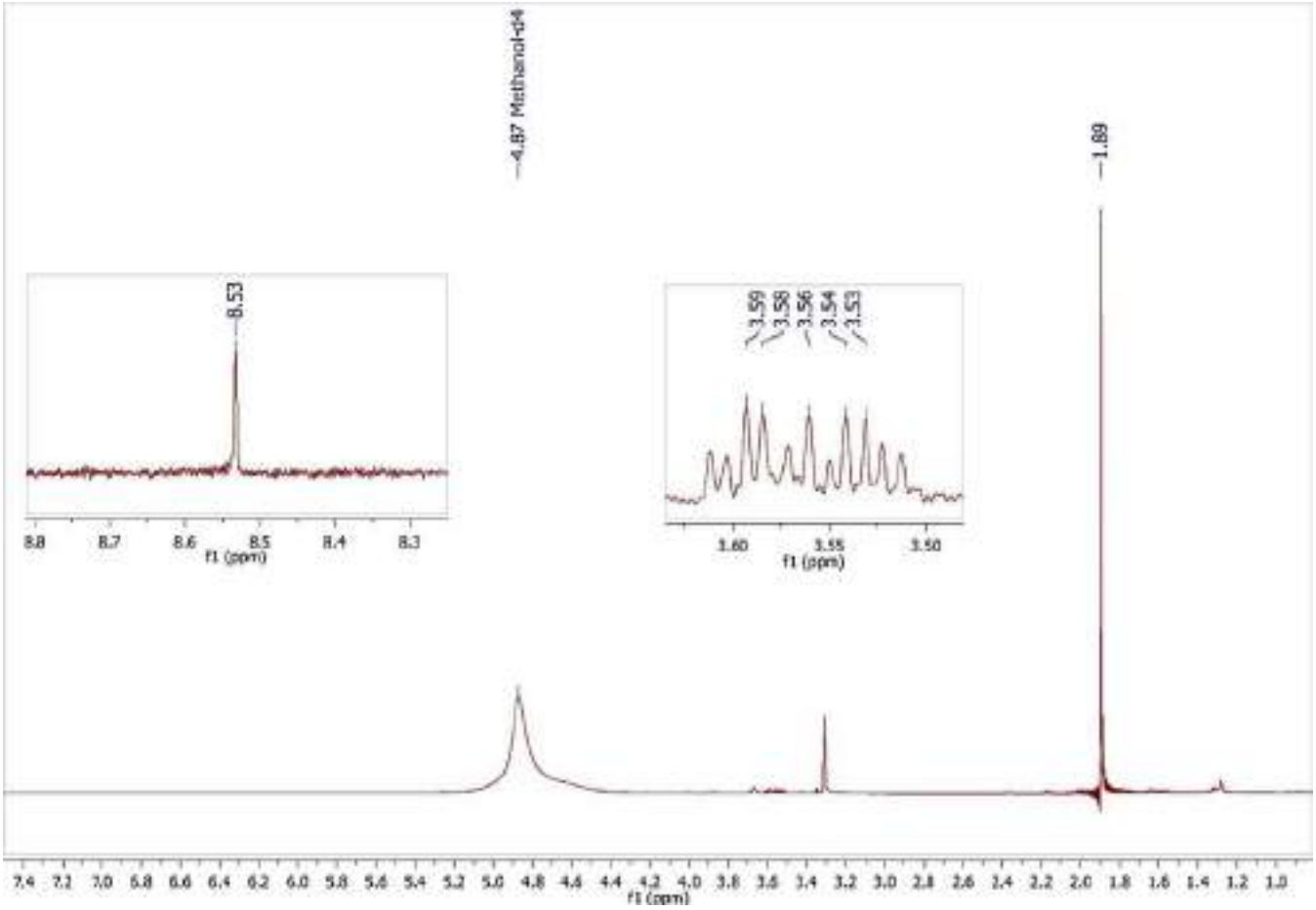

Fig. 17. ^{1}H NMR of the washes of hydrogel with NaOH and distilled water.

the crosslinking agent. The author found a decrease in pore size for hydrogels having a higher concentration of gallic acid [33]. Lenka Musilová also reported that the hydrogel content of the crosslinking agent, in this case lignin, influenced the porosity of the material [34].

3.8. Swelling

The degree of swelling of the material was determined by the quantity of water absorbed by the hydrogel. The percent of swelling was calculated as a function of the time the material was immersed in water, using hydrogels with 2, 6 and 10 wt% of GA (Fig. 16). The results reveal that the degree of cross-linking strongly influenced the swelling volume. A greater degree of swelling was found in the material having a higher versus lower percentage of the crosslinking agent (10 versus 2 wt.%, respectively). Accordingly, the hydrogels containing 10 wt% GA absorbed 60% of water in the first 1.5 min, while the materials with 2 wt% only absorbed 20%. The enhanced capacity to trap water is attributed to the greater flexibility of the polymer with a higher concentration of GA. [35] The maximum water absorption per gram of hydrogel at the different concentrations of GA illustrates this point (Table 5).

A gram of hydrogel containing GA at 2 wt.% absorbed 5.83 g of water, almost 6 times its weight while a gram of hydrogel with 10 wt.% of GA had a maximum absorption of 30.51 g of water, corresponding to 30 times its weight.

This phenomenon was reported by Ming Fan and co-workers [36], who experimented with polysaccharide hydrogels derived from CS and hyaluronan via a metal-free Click reaction. They investigated the swelling behavior of hydrogels and concluded CS and hyaluronic acid have an abundant number of hydrophilic groups (e.g., hydroxyl, amino and carboxyl groups), which allow for robust hydration.

3.9. Cytotoxicity assay

Extracted GA traces obtained during the washing were quantified (Table 6) and analyzed by NMR. The ^{1}NMR spectra shows a peak at 8.53 ppm of protons presents in GA, demonstrating that non-crosslinked GA was removed (Fig. 17). The results show that hydrogels with 8 and 10 wt %GA, presented the higher concentrations of residual GA.

The cytocompatibility of CS-GA hydrogels with human fibroblasts was evaluated by using a live/dead cytotoxicity assay. The cells were seeded on the hydrogels and left for three days at 37 °C. Subsequently, the hydrogel platforms were stained with calcein/ethidium homodimer for the visualization of viable cells under an optical microscope (Fig. 18).

Viable fibroblasts were clearly seen in the platforms containing 2, 4 and 6 wt.% GA, indicating cytocompatibility at those concentrations. Viable cells can be appreciated alone or clusters, both on the surface of hydrogels. The hydrogels with GA at 8 and 10 wt% did not display cell viability, cells could not adhere perhaps due to the higher concentration of GA.

The percentage of cell viability of fibroblast was determined by

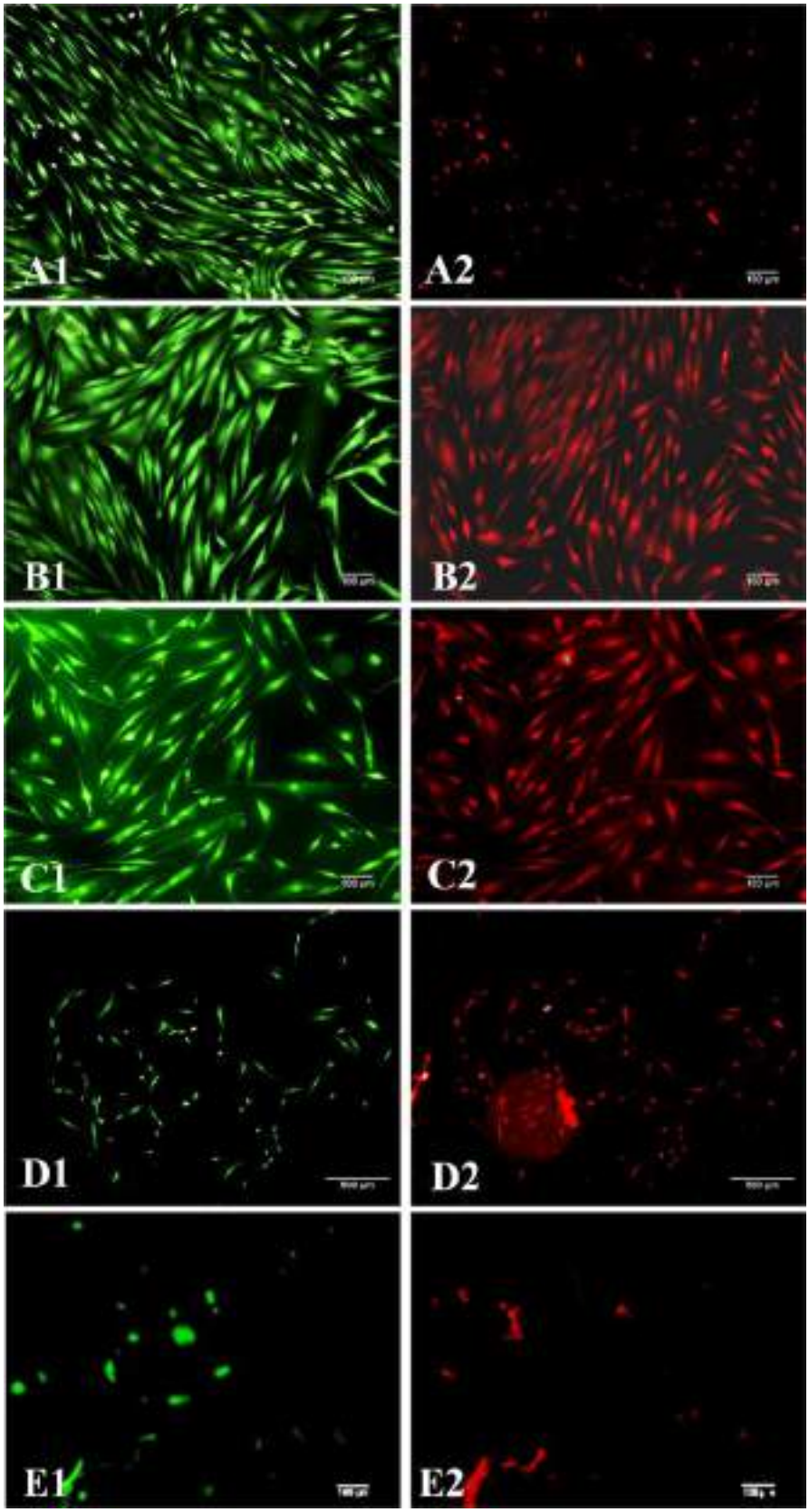

Fig. 18. Fluorescence micrographs of the fibroblast cells onto hydrogels with the crosslinking agent at 2 wt% (A), 4 wt% (B), 6 wt% (C), 8 wt% (D) and 10 wt% (E). Live cells are visible as green (1), dead cells are observed as red (2) (For interpretation of the references to colour in this figure legend, the reader is referred to the web version of this article).

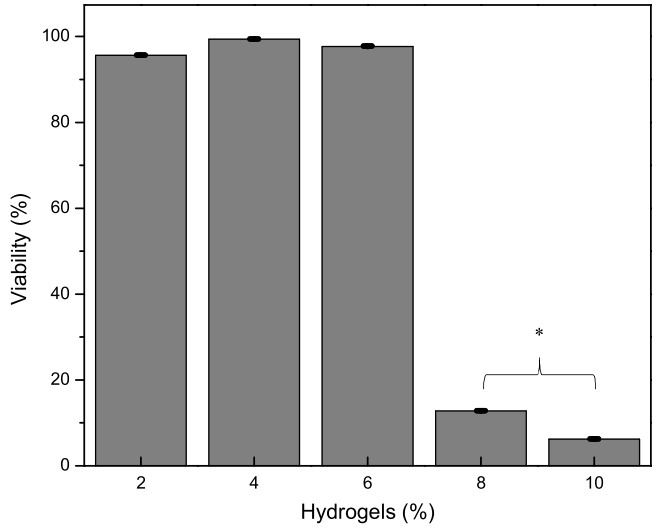

Fig. 19. Viability of fibroblasts after 3 days incubation at 37 °C with hydrogels with different degrees of crosslinking. Asterisk denote significant difference compared with hydrogels at 2 wt%, 6 wt% and 10 wt% of GA * p, 0.01.

imagine analysis (Fig. 19) It observes that hydrogels with 8 and 10% of GA ($\sigma = 3.22$) were cytotoxic, while hydrogels with 2, 4 and 6% ($\sigma = 1.57$) are the best candidates showed above 95% cells survival, attributed to the low concentration of GA, confining the results of fluorescence microscopy.

The seeded hydrogels were observed by SEM in order to determine where the cell growth takes place (Fig. 20). The micrographs showed cells adhere on the surface of the hydrogel, exhibiting a typical elongated and spindle-like morphology. It is also observed that the orientation of the fibroblasts is not parallel, attributing to the multilayer of cells on the hydrogel. That means that the cells grow one on top of the other to produce superimposed layers of cells of different orientation. [37]

4. Conclusions

Novel hydrogels were synthesized by using Schiff reactions to crosslink CS with GA. Hydrogels having different concentrations of GA were tested to determine the effect on swelling and rheological properties. Examination was made of the degree of crosslinking bond formation (with TGA-DA) and of the presence of residual GA in the uncrossed part (with NMR). The reaction kinetics and reaction order, assessed with UV–vis spectroscopy, showed a pseudo cero order for the reaction. Moreover, the constant rate values were dependent on the concentration of GA. The rheological properties evidenced a decrease in the strain strength when a more rigid network was formed. There was a significant increase in the swelling capacity of the material with greater GA content, finding the best water absorption capacity at 10 wt%. However, only the hydrogels at 2, 4 and 6 wt% were cytocompatible. The present results suggest that hydrogels consisting of CS cross-linked with GA could possibly provide an adequate scaffold for tissue engineering. Further research is needed to explore the *in vivo* plausibility of such a scaffold.

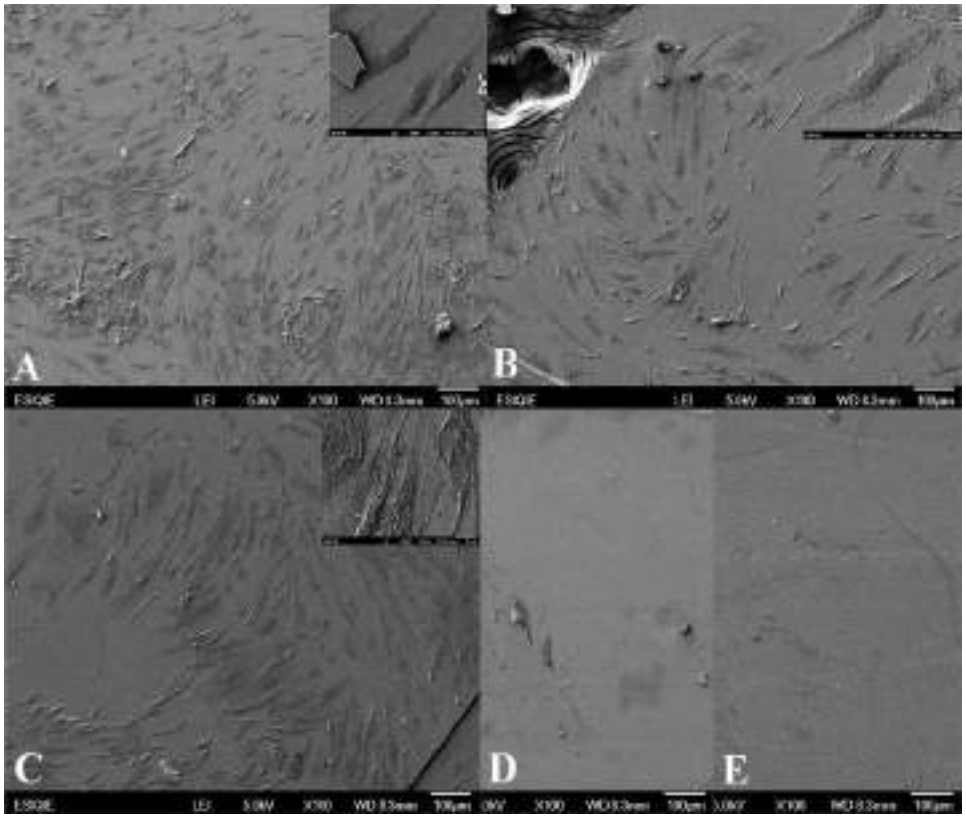

Fig. 20. SEM images of the fibroblast cells onto hydrogels with the crosslinking agent at 2 wt% (A), 4 wt% (B), 6 wt% (C), 8 wt% (D) and 10 wt% (E).

Acknowledgements

This project was supported by grant from the Consejo Nacional de Ciencia y Tecnología (CONACYT, grant # 743999). The authors would like to acknowledge the help of Dr. Hugo Martínez Gutierrez in carrying out the SEM assay, and of Dr. Daniel Arriéta Baez in performing the HR-MS at the Centro de Nanociencias y Micro-nanotecnologías. Finally, we thank Dr. Jose Antonio Serrato Pérez of the Instituto Nacional de Enfermedades Respiratorias (INER).

Appendix A. Supplementary data

Supplementary material related to this article can be found, in the online version, at doi:https://doi.org/10.1016/j.colsurfa.2019.123658.

References

[1] T.S. Demina, D.S. Zaytseva-Zotova, T.A. Akopova, A.N. Zelenetskii, E.A. Markvicheva, J. Appl. Polym. Sci. 134 (2017) 17–19.
[2] N. Scaplehorn, Cell 149 (2012) 727–729.
[3] S. Kim, T. Kawai, D. Wang, Y. Yang, ACS Appl. Mater. Interfaces 8 (2016) 19245–19255.
[4] R. Jin, L.S.M. Teixeira, A. Krouwels, P.J. Dijkstra, C.A. Van Blitterswijk, M. Karperien, J. Feijen, Acta Biomater. 6 (2010) 1968–1977.
[5] K.Y. Lee, D.J. Mooney, Chem. Rev. 101 (2001) 1869–1879.
[6] S. Ahadian, R.B. Sadeghian, S. Salehi, S. Ostrovidov, H. Bae, M. Ramalingam, A. Khademhosseini, Bioconjug. Chem. 26 (2015) 1984–2001.
[7] J.A. Yang, J. Yeom, B.W. Hwang, A.S. Hoffman, S.K. Hahn, Prog. Polym. Sci. 39 (2014) 1973–1986.
[8] D.G. Miranda, S.M. Malmonge, D.M. Campos, N.G. Attik, B. Grosgogeat, K. Gritsch, J. Biomed. Mater. Res. - Part B Appl. Biomater 104 (2016) 1691–1702.
[9] M. Ray, K. Pal, A. Anis, A.K. Banthia, Des. Monomers Polym 13 (2010) 193–206.
[10] S.J. Buwalda, K.W.M. Boere, P.J. Dijkstra, J. Feijen, T. Vermonden, W.E. Hennink, J. Control. Release 190 (2014) 254–273.
[11] R. Santillán, E. Nieves, P. Alejandre, E. Pérez, J.M. Del Río, M. Corea, Colloids Surfaces A Physicochem. Eng. Asp 444 (2014) 189–208.
[12] X.Z. Shu, Y. Liu, F.S. Palumbo, Y. Luo, G.D. Prestwich, Biomaterials 25 (2004) 1339–1348.
[13] M.B. Thürmer, C.E. Diehl, F.J.B. Brum, L.A. dos Santos, Mater. Res 17 (2014) 109–113.
[14] J. Kopeček, Biomaterials 28 (2007) 5185–5192.
[15] L.E. Jansen, L.J. Negrón-Piñeiro, S. Galarza, S.R. Peyton, Acta Biomater. 70 (2018) 120–128.
[16] R.M. Desai, S.T. Koshy, S.A. Hilderbrand, D.J. Mooney, N.S. Joshi, Biomaterials 50 (2015) 30–37.
[17] A.R. Karimi, B. Rostaminejad, L. Rahimi, A. Khodadadi, H. Khanmohammadi, A. Shahriari, Int. J. Biol. Macromol. 118 (2018) 1863–1870.
[18] T.K. Giri, A. Thakur, A. Alexander, Ajazuddin, H. Badwaik, D.K. Tripathi, Acta Pharm. Sin. B 2 (2012) 439–449.
[19] C. Arakawa, R. Ng, S. Tan, S. Kim, B. Wu, M. Lee, J. Tissue Eng. Regen. Med. 11 (2017) 164–174.
[20] F. Croisier, C. Jérôme, Eur. Polym. J. 49 (2013) 780–792.
[21] J. Duan, X. Liang, Y. Cao, S. Wang, L. Zhang, Macromolecules 48 (2015) 2706–2714.
[22] H.M. Franzén, K.I. Draget, J. Langebäck, J. Nilsen-Nygaard, Polymers 7 (2015) 373–389.
[23] M. Shivashankar, B.K. Mandal, R. Yerappagari, V.P. Kumar, Int. Res. J. Pharm. Pharmacol. 2 (2011) 1–6.
[24] R.B. Seligman, J. Org. Chem. 285 (1960) 228–232.
[25] H. Akin, N. Hasirclt, J. Appl. Polym. Sci. 58 (1995) 95–100.
[26] L. Liao, H. Yue, Y. Cui, Chinese J. Chem. Eng 19 (2011) 285–291.
[27] A. Maria Marzaioli, E. Bedini, R. Lanzetta, V. Perino, M. Parrilli, C. De Castro, Carbohydr. Polym. 90 (2012) 847–852.
[28] J. Mourycová, K.K.R. Datta, A. Procházková, M. Plotěná, V. Enev, J. Smilek, J. Másílko, M. Pekař, Int. J. Biol. Macromol. 111 (2018) 680–684.
[29] E.T.J. Klompen, Mechanical Properties of Solid Polymers: Constitutive Modelling of Long and Short Term Behaviour, Eindhoven: Technische Universiteit Eindhoven, (2005) 141p..
[30] Thangavel, B. Ramachandran, V. Muthuvijayan, J. Biomed. Mater. Res. - Part B Appl. Biomater. 104 (2016) 750–760.
[31] M. Kim, J.Y. Lee, C.N. Jones, A. Revzin, G. Tae, Biomaterials 31 (2010) 3596–3603.
[32] Fernandez-Tresguerres Hernandez-Gil, M.A. Alobera Gracia, M. Del Canto Pingarrón, L. Blanco Jerez, Med. Oral Patol. Oral Cir. Bucal 11 (2006) 32–36.
[33] Stefanov, S. Pérez-Rafael, J. Hoyo, J. Cailloux, O.O. Santana Pérez, D. Hinojosa-Caballero, T. Tzanov, Biomacromolecules 18 (2017) 1544–1555.
[34] L. Musilová, A. Mráček, A. Kovalcik, P. Smolka, A. Minařík, P. Humpolíček, R. Vícha, P. Ponížil, Carbohydr. Polym. 181 (2018) 394–403.
[35] F. Reyes Ortega, G. Rodríguez, M. Rosa Aguilar, J. García-Sanmartín, A. Martínez, J. San Román, Biomecnica 20 (2012) 7–19.
[36] M. Fan, Y. Ma, J. Mao, Z. Zhang, H. Tan, Acta Biomater. 20 (2015) 60–68.
[37] B. Sarker, R. Singh, R. Silva, J.A. Roether, J. Kaschta, R. Detsch, D.W. Schubert, I. Cicha, A.R. Boccaccini, PLoS One 9 (2014) 1–12.